Aerothermodynamic Design Feasibility of a Mars Aerocapture Vehicle

Dwight E. Florence*
General Electric Company, Philadelphia, Pennsylvania

Lifting aerodynamic configurations have been screened and selected for the Mars aerocapture mission that meet the geometric packaging requirements of the various payloads and the Space Shuttle cargo bay and provide the aerodynamic performance characteristics required to obtain the atmospheric exit steering accuracy desired. Hypersonic heat transfer and aerodynamic loads to the vehicle in the CO_2 atmosphere are evaluated. Contemporary low-density ablative thermal protection materials were selected that met all the atmospheric entry requirements and provide a minimum mass solution. Results of the aerodynamic configuration and thermal protection materials screening and selection are presented. It is concluded that the aerothermodynamic design of the concept is feasible using state-of-the-art technology.

Nomenclature

A = reference (base) area, m^2
C_D = drag coefficient
C_L = lift coefficient
C_N = normal force coefficient
C_m = coefficient of pitching moment
h = altitude, km
L/D = lift-to-drag ratio
L_A = apex length of vehicle, meters
$\dot{q}$ = local heat transfer rate, w/cm^2
Re_θ = Reynolds number based on local properties and momentum thickness
Re = freestream Reynolds number
R_I = intermediate radius of vehicle,
R_B = base radius, m
R_N = nose radius, m
SM = single mission
TPS = thermal protection system
V = inertial velocity, m/s
W = weight of vehicle, kg
X = axial distance, m
X_{CG} = center of gravity location, m
X_{CP} = center of pressure location, m
α = angle of attack
α_T = trim angle of attack
δ_N = nose bend angle, deg
γ = air relative flight path angle at entry
ρ = material density, kg/m^3
θ = cone angle, heating time, s

Subscripts

∞ = Freestream conditions
S = stagnation point
CIRCULAR = circular satellite velocity at that altitude

Introduction

PLANETARY missions have historically employed near minimum energy trajectories in order to maximize payload delivered to the planets. As a consequence, trip times have been near the maximums and mission launch windows somewhat limited. The typical mission scenario is a chemically fired kick stage for braking from the approach trajectory into a capture orbit about the target planet. Recently, aerodynamic braking/capture techniques have been evaluated, significantly increasing payload weight[1,2] or reducing transit time. The aerocapture technique employs both lift and drag to affect the capture, whereas the aerobrake technique employs only drag.

Aerocapture is particularly attractive for the Mars Sample Return Mission, where it has been estimated that the lander and orbiter to be captured into Mars orbit weigh almost 4000 kg.[3] If chemical propulsion were used for orbit insertion, the trans-Mars payload weight would be more than double the orbiter/lander 4000 kg mass. This far exceeds the maximum space shuttle/twin stage inertial upper stage (IUS) capability of 5100 kg for a 1988 launch. This paper describes the selection and development of a one-pass aerocapture configuration and its thermal protection system (TPS).

The major phases of the approach, entry, capture, and exit portions of the mission are illustrated in Fig. 1. Prior to atmospheric entry, the vehicle is positioned in a generally nose forward attitude. As the aerodynamic forces build up, the vehicle moves naturally to the preselected trim angle of attack. The plunge of the vehicle into the planetary atmosphere is arrested, employing full lift up, whereupon a roll maneuver is

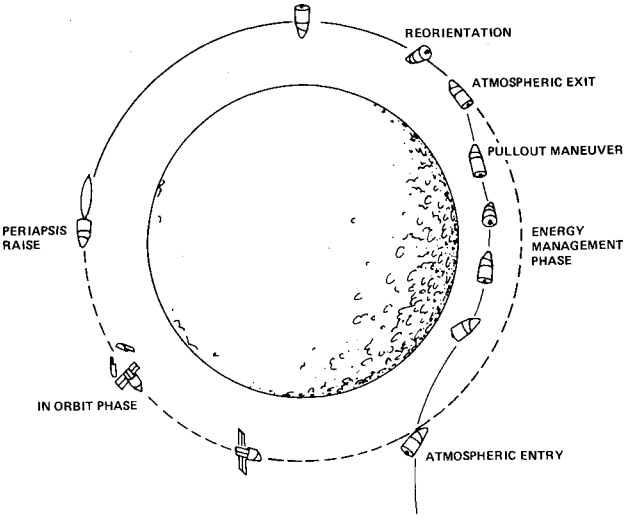

Fig. 1 Aerocapture sequence of events.

Presented as Paper 81-0350 at the AIAA 19th Aerospace Sciences Meeting, St. Louis, Mo., Jan. 12-15, 1981; received March 6, 1981; revision received Jan. 10, 1984.

*Staff Engineer, Re-entry Systems Technology. Member AIAA.

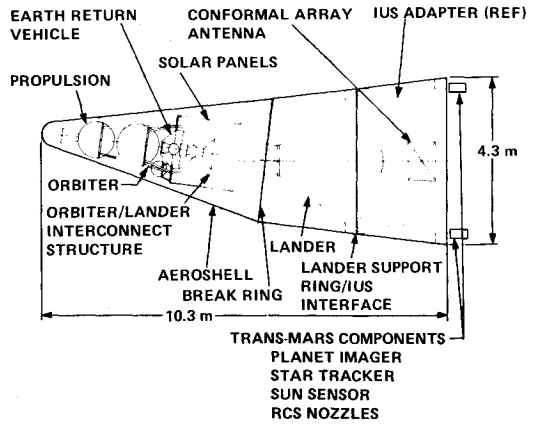

Fig. 2 Selected SM vehicle configuration.

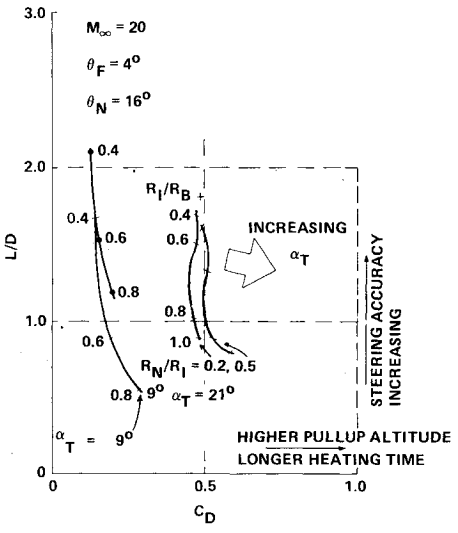

Fig. 3 Existing biconic data base.

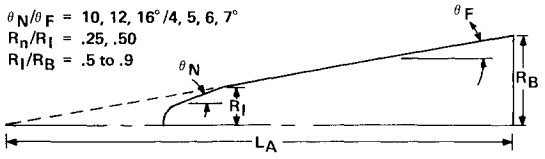

Fig. 4 Initial vehicle basic body screening matrix.

initiated to nearly full lift down after the preselected deceleration rates are reached. With the vehicle flying at a fixed trim angle of attack, the lift vector is roll modulated to hold a constant deceleration rate until the inertial velocity approaches $V_{circular}$. At that time, the vehicle is rolled back to full lift up and lofts out of the atmosphere. On reaching apoapsis, a small propulsive burn raises periapsis out of the atmosphere.

Aerocapture vehicle configurations were developed for two specific Mars Sample Return mission modes.[1,3] In the single mission mode (SM), the aerocapture vehicle is required to perform aerocapture into Mars orbit only. The aeroshell must package an orbiter and a completely autonomous Viking type lander, Fig. 2. The aeroshell is separated from the orbiter/lander combination between the aerocapture and the periapsis raise maneuver. In the multi-mission mode (MM), the aeroshell must perform not only the aerocapture into Mars orbit, but its forward portion (integrated with the lander subsystems) must also perform the final entry from orbit to parachute deployment (referred to as the aeromaneuver portion), where the lander is released. This paper will discuss only the single mission vehicle.

Aerodynamic Configuration

Aerodynamic Configuration Screening Approach

The configurations selected for the Mars SM aerocapture vehicle must make it capable of packaging the required payloads, fitting within the length and width constraints of the Space Shuttle payload bay, and providing a lift to drag ratio of between 1 and 2 and a drag coefficient of between 0.4 and 1.0 to meet the steering accuracy requirement as specified in Ref. 3.

Several classes of configurations exist that meet these hypersonic performance requirements, axisymmetric and elliptical cross-section cones, biconics, and arbitrary cross-section bodies. Generally, cones are too long to meet the Space Shuttle payload bay length constraint and package the required payloads. Arbitrary bodies have generally been designed with other mission requirements in mind, (e.g., higher hypersonic lift-to-drag ratio (L/D) or subsonic landing capability) and thus are geometrically more complex than necessary for this aerocapture/aeromaneuver vehicle. The class of configuration that most readily lends itself to the packaging constraints is axisymmetric biconic. Biconics can be trimmed at an angle of attack by a variety of control techniques including c.g. offset, bent nose, aft frustum slice, or flaps. Perhaps the least complex concept is that of a fixed bent nose, which provides a nearly fixed trim angle of attack and the bank to turn steering approach.

The three-dimensional flowfield (3DFF) capability has been used to provide accurate and rapid estimates of the aerodynamic characteristics of candidate maneuvering aerocapture vehicle configurations for use in the mission/trajectory simulations. The 3DFF system consists of two primary codes: a three-dimensional inviscid code (3IFF)[4] and a three-dimensional viscous code (3VFF).[5] The 3IFF code is used to compute surface pressures and shock shape for various multiconic body geometries, including asymmetric noses, bent nose bodies, and aft slices. The 3VFF code considers viscous-inviscid interaction, mass addition from the thermal protection system, asymmetric boundary layer transition in the pitch and yaw planes, and real gas characteristics. Aerodynamic coefficients are computed, including inviscid flow contributions to forces and moments and the viscous contributions caused by induced pressure and skin friction. The 3VFF code is also used to predict the aerothermodynamic environment of the entry configurations. The aerocoefficients of the selected configurations have been evaluated in CO_2 with real gas effects included.

The hypersonic arbitrary body computer program (HABP),[6] has been employed to determine the aerodynamic characteristics of the candidate vehicles at very high angles of attack (> 20 deg).

A data bank of 3DFF results exists for biconics in Fig. 3, and is compared to the L/D and C_D range required for the Mars aerocapture vehicle. Although some separated flow is expected on the leeward side, the pressures there are quite low; therefore, it is anticipated that the windward pressures dominate and no significant shift in C_D or C_L occurs with separation onset at the higher angles of attack.

The initial array of acceptable single-mission vehicle basic bodies was selected to meet several criteria including allowable length, yaw, and pitch stability considerations, and L/D and C_D requirements.

Single Mission Vehicle Selected

The specific range of configuration parameters surveyed is illustrated in Fig. 4. Thirteen specific configurations were

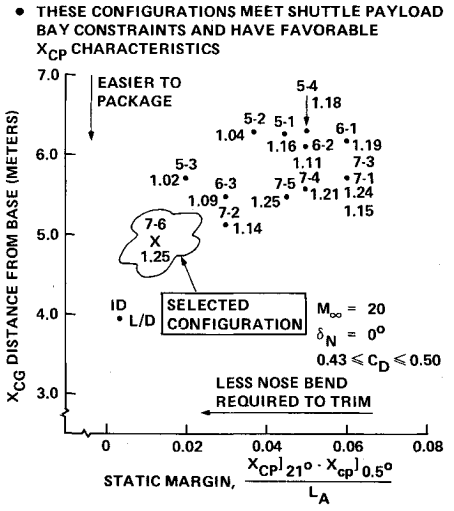

Fig. 5 Results of initial screening process.

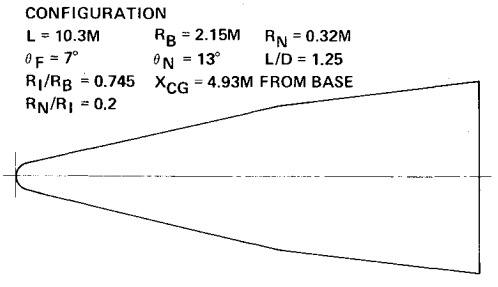

Fig. 6 Selected vehicle basic body.

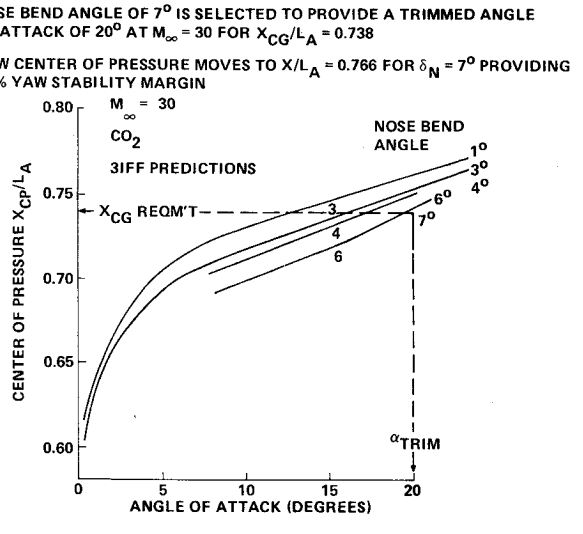

Fig. 7 Effect of nose bend angle on axial and normal force coefficients.

examined that met the initial screening criteria. The trends of axial c.g. requirements and an estimate of nose bend required to trim the vehicle are summarized for these thirteen configurations in Fig. 5. The configuration selected for further evaluation was Number 7-6. This configuration provided the furthest aft c.g. location requirement to hold the trim angle and thus is easier to package. It also had the highest L/D and displayed the minimum static margin, which is proportional to the nose bend angle required to trim the vehicle at the desired

Table 1 Aerodynamic characteristics summary of selected configuration

	Flow State	
Characteristic	Laminar	Turbulent
α trim	20	20
L/D	1.160	1.026
C_D	0.481	0.522

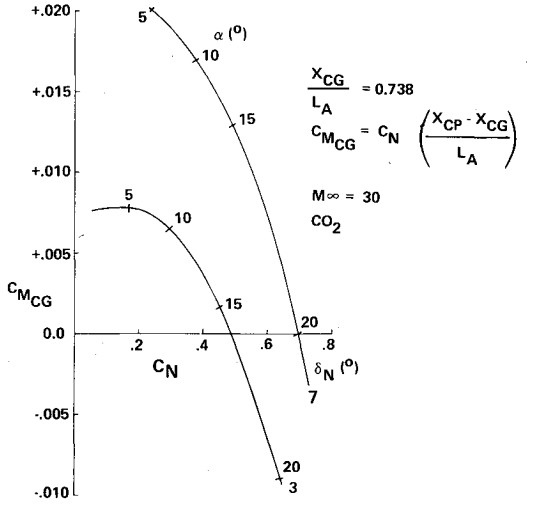

Fig. 8 Longitudinal stability characteristics.

angle of attack. Specific characteristics of this selected configuration are illustrated in Fig. 6.

The aerodynamic characteristics screened to this point are for zero nose bend (since nose bend is usually a second-order effect on C_L, C_D, L/D and $X_{CG_{REQ'D}}$) and a flight medium of air. Calculations have been made for the selected configuration using the 3IFF code to determine the effect of nose bend angle on the axial center of pressure location in the pitch plane and thus determine the nose bend angle required to produce the desired trim angle of attack. An axial c.g. location of 0.738 L_{apex} with a nose bend angle of 7 deg results in a trim angle of 20 deg while maintaining a very adequate (by standard design practice) yaw stability margin of 2.8%. Axial and normal force coefficient variations with nose bend angle and angle of attack are illustrated in Fig. 7 and summarized at the trim angle in Table 1. Longitudinal stability characteristics for the configuration with a selected nose bend angle of 7 deg are illustrated in Fig. 8. This configuration provides a pitch stability margin at the 20 deg trim angle of 8.4%.

Entry/Heating Thermal Protection Subsystem (TPS)

A state-of-the-art, minimum-mass TPS that meets all atmospheric entry requirements was selected for the aerocapture vehicle. Since the mass of the TPS and its supporting substructure is a major portion of the aerocapture/aeromaneuvering vehicle, selection of a minimum-mass TPS concept greatly enhances the potential science return benefits of the aerocapture mission concept.

The requirements to be placed on the TPS include the following: high thermal efficiency to meet mass and thickness goals, meet JSC vacuum outgassing requirements, and meet the planetary quarantine conditions.

Aerothermodynamic Design Approach

Hypersonic heat transfer distribution and heat protection material thickness requirements have been computed using the

3VFF[5] code and design correlations generated with the REKAP design code.[7]

The onset of local turbulent flow, which results in approximately doubling local laminar heat transfer rates, was based on available flight test transition data correlations analytically scaled to the Aerocapture vehicle geometry. The thermal protection material thickness was sized to limit the maximum bondline temperature to 316°C (600°F) for an RTV bond thickness of 0.46 mm (0.018 in.), a contemporary design practice based on bond strength degradation. Typically, during the period of maximum entry loads, the bond and structure are at room temperature and reach their peaks during the long soak out after the heating period is over. TPS requirements were evaluated considering nominal trajectories and a nominal initial temperature of 38°C (100°F).

The heating rates to the aerocapture vehicle frustum sections have been calculated for selected configurations by means of the three-dimensional viscous boundary layer code (3VFF). This program calculates the Eckert Reference Enthalpy and Vaglio-Laurin laminar, transitional, and turbulent heating rate distributions, as well as skin friction and viscous drag over sphere-cone and biconic configurations at angle of attack. The code uses integral boundary layer techniques, including entropy swallowing effects, along boundary layer edge loci computed on the basis of the local pressure gradient. The inviscid flow field pressure and shock shape are obtained from data generated by the three-dimensional flow field program (3IFF).[4]

A cursory evaluation of off-nominal aerocapture trajectories indicated that considering a range of entry angles from −14.5 to −16.5 deg and the range of atmosphere models from minimum to maximum density, the most severe combination for sizing the thermal protection system is minimum path angle into the minimum density atmosphere model. This entry results in heating loads and heating times slightly higher than those experienced for nominal path angle (−15.5 deg) entry into the mean density atmosphere. Local thermal protection material requirements increased by 4 to 14% for the worst case, off-nominal aerocapture. These increases are small, can be covered by addition of a thermal safety margin to the nominal requirements, and are well within allowable launch weights.

Hypersonic Heat Transfer During Aerocapture

The hypersonic heat transfer magnitude during aerocapture is strongly dependent upon the configuration geometry and size, and the steering algorithm employed.

A series of initial 3DOF trajectory calculations have been made for the aerocapture portion of the mission[1] for a range of possible vehicle characteristics. Included in these simulations were approximations for calculations of hypersonic heat transfer to a vehicle stagnation point and calculation of freestream Reynolds Number. Results of these calculations are summarized in Fig. 9. The duration of the heat pulse (Θ), which also drives the thermal insulation requirement, varies from 310 to 500 s. Peak stagnation point, heat transfer rate, and heat load for several candidate single mission vehicles are summarized in Table 2. Typical local heat transfer distributions over the single mission aerocapture vehicle are illustrated in Fig. 10. Note that a significant increase in heat transfer rate occurs as the local flow trips to turbulent. The boundary layer transition criterion employed was a recently published Re_θ criterion.[8] Employing this correlation, probable turbulent windward and side ray meridians are predicted.

Thermal Protection Material Selection

A number of thermal protection materials have been examined in TPS thickness-weight tradeoffs. These materials have various ablative, insulative, and reusable characteristics that can provide different design advantages for these lifting entry missions, depending upon the trajectory steering option selected. Generally, a material will be selected that experiences little or no shape change, with most of the thickness employed

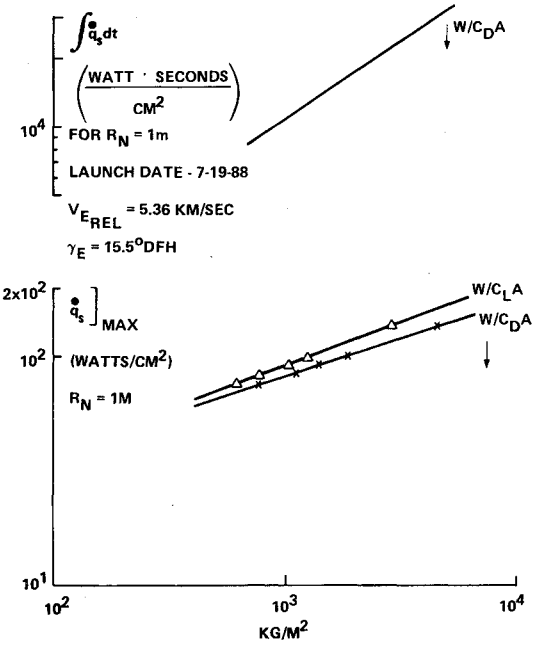

Fig. 9 Effect of lift or drag loading on peak stagnation point heat transfer.

Table 2 Summary of heating parameters normalized to a 5000# KG aerocapture vehicle

Parameter	Vehicle 7-6	7-8	7-10
C_D	0.49	0.44	0.44
A_{Base}, m²	14.5	8.0	10.2
W/C_DA, kg/m²	704	1120	1410
$\dot{q}_{max_{stag}}$, W/cm²	127	166	153
$\int \dot{q}s\, dt$, W/cm² − s	14,500	24,282	20,448
Heating time, s	310	350	322

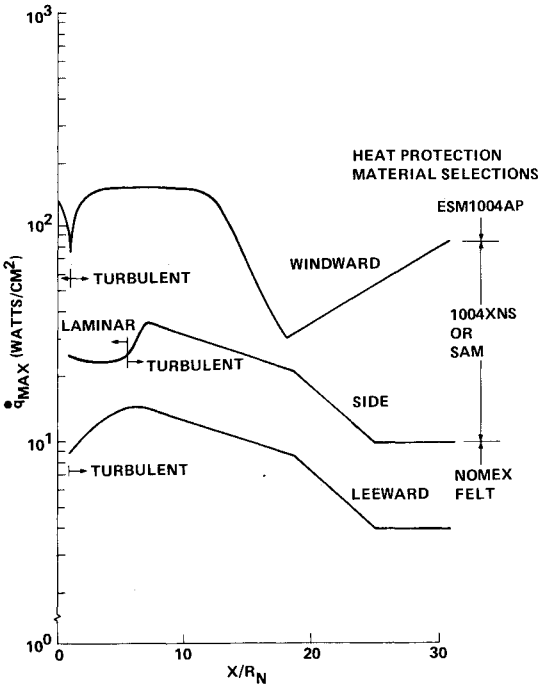

Fig. 10 Peak heat transfer rates.

Table 3 Comparison of candidate material thermophysical properties

Material	Density, kg/m^3	Thermal conductivity, W/m°K	Specific heat, cal/gm°K
ESM1004LPS	880	1.82×10^{-1}	0.31
ESM1004AP	575	1.48×10^{-1}	0.31
ESM1004X	240	9.66×10^{-2}	0.355
SAM	128	4.43×10^{-2}	0.228
Nomex Felt	83	4.80×10^{-2}	0.49

to provide insulation to the bond and structure. The candidate material systems fall into several broad categories and include reusable surface insulation (RSI) bonded to a structure, reusable reradiative metallic panels backed by low-density insulation, and low-density ablator or insulator panels bonded to the structure. These materials have various areas of desirability, applicability, and attractiveness, depending on the heat rates and heat loads experienced by the vehicle.

Locally on the aerocapture vehicle, peak heat transfer normally occurs near pullup. The magnitude of the local peak heat transfer rate usually drives the selection of the thermal protection material. Materials such as RSI or reradiative metallic panels have maximum allowable temperatures, whereas low-density ablators such as ESM have higher heat flux thresholds above which char recession is experienced. The RSI and reradiative metallic cover panels are most attractive for low heat flux areas where peak heat fluxes are limited to 44 and 25 W/cm^2, respectively. A review of Fig. 10 indicates that RSI and metallics would be applicable only to the vehicle side and leeward areas. Low-density charring ablators, such as ESM 1004[9] and SAM[10] are more attractive for the higher heat flux areas displayed on the windward and side areas.

A filled, foamed, silicone, elastomeric shield material (ESM) has been fabricated, tested, and flown in a range of material densities ranging from 240 to 880 kg/m^3.[9] The lower density ESM, 1004XNS, is the most thermally efficient (lower $k\rho$) of the ESM series,[11] Table 3. Another very attractive low density ablator is Silicone Ablative Material (SAM). Development of this material, a derivative of silica Reusable External Insulation (REI)[12] was sponsored in 1973.[10] These materials (both the ESM series and SAM) have melt thresholds that have been identified in plasma arc ground tests.[9,10] The only materials whose performance have been characterized in the melting regime are ESM 1004AP and 1004LPS.[9] ESM 1004XNS and SAM are recommended for use only in the no-melt shape stable mode. The upper limit of heat transfer rate recommended for ESM 1004XNS and SAM is 86 W/cm^2.

In the cooler area of the leeward side ($\dot{q} < 10$ W/cm^2), a lower density material like the room temperature vulcanizing (RTV) coated Nomex felt being used on the top side of the Space Shuttle is very weight attractive, because of its excellent thermal properties. This material is considered to be reusable at temperatures up to 450°C (850°F), and with supporting test data available for the purposes of this study, has been considered usable for aerocapture for peak surface temperatures of 540°C (1000°F) and heat transfer rates up to 10 W/cm^2.

TPS thickness requirements have been generated for these selected materials. The significant weight trade driving the material selection is illustrated in Fig. 11 for several candidate ablators on the windward and leeward sides of the single mission vehicle. The summary of local heat load distributions, local thermal protection material selected, and local TPS weight requirement is presented in Table 4 and illustrated in Fig. 12.

The hypersonic heat transfer experienced during aerocapture is well into the continuum flow regime, and reaches peak load and rates that cover the range that has been experienced in out-of-orbit earth entry flight testing of ballistic satellites

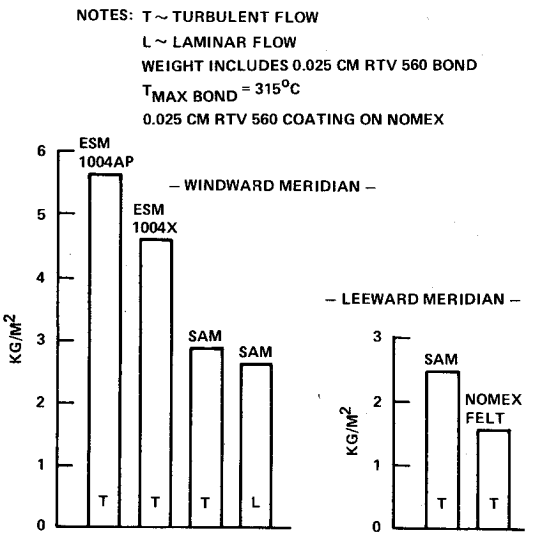

Fig. 11 Aft frustum TPS comparison.

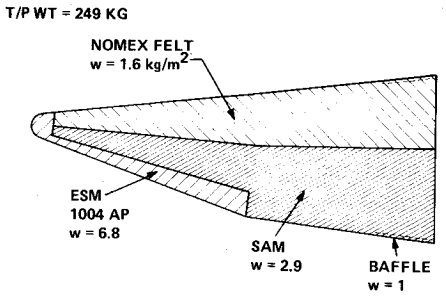

Fig. 12 Thermal protection material selection and arrangement.

and the to-be-tested Space Shuttle. Employing recent correlations of flight test boundary layer transition data, turbulent flow is expected to prevail over most of the vehicle at pull up during the aerocapture portion of entry. The thermal protection was sized for a nominal entry consistent with a July 1988 launch opportunity, an entry relative velocity = 5.4 km/s, and path angle = 15.5 deg.

Summary

Potential maneuvering vehicle basic body candidates have been screened for the Single Mission vehicle considering the packaging constraints and the desired aerodynamic performance characteristics. A basic biconic body was selected, Fig. 6, based on meeting the aerodynamic characteristics requirements, ease of packaging the given payloads in the vehicles and the vehicles in the Space Shuttle payload bay, minimizing the nose bend required to trim the vehicle, minimizing the vehicle surface area where possible, and providing some degree of longitudinal and directional static stability.

The Single Mission vehicle configuration selected is driven by the large diameter of the Viking Lander, Fig. 2, and the Space Shuttle payload bay diameter constraint. Adding now the Space Shuttle bay length constraint, the maximum L/D of this configuration is limited. The minimum drag coefficient goal of ≥ 0.4 is met by selecting a vehicle trim angle of attack of 20 deg. This results in aerodynamic characteristics at the trim angle of attack of $C_D = 0.52$ and $L/D = 1.03$, Table 1.

Dominant flow regime for the vehicle is continuum flow with turbulent flow present over most of the vehicle at pull up. Aerodynamic characteristics defined have considered the inviscid, skin friction, and induced pressure effects, although only the inviscid effects are of the first order.

Table 4 Thermal protection system requirements summary

Vehicle station, m	Peripheral location, deg	$\int \dot{q}\,dt$ W/cm^2	Material selection	Unit weight kg/m^2
STAG	0	14495	ESM1004AP	6.4
1.6	0	22052	ESM1004AP	6.9
4	0	18901	ESM1004AP	6.7
4.5	0	12600	SAM	2.9
10.3	0	12600	SAM	2.8
1.8	90	2754	SAM	2.6
5.9	90	3150	SAM	2.6
10.3	90	1470	SAM	2.5
5.9	180	1260	Nomex Felt	1.6

A combination of several low-density ablators has been selected to provide a minimum mass thermal protection system that meets all the requirements of the aerocapture vehicle. Low density ablators were selected over a metallic reradiative type or an RSI approach due to the limited reuse required, simplicity of design, fabrication, applications, data base existing, and cost.

In the nose and windward forward frustum areas where the peak heat transfer rates range from 86 to 200 W/cm^2, ESM 1004AP has been selected. Further aft, where the rates range from 10 to 86 W/cm^2, the lower density ablators such as ESM 1004XNS or SAM are recommended; on the leeward side where the rates peak at 10 W/cm^2 or less, the Nomex felt employed on the leeward side of the Space Shuttle is recommended. Local thermal protection concepts are illustrated in Fig. 12. Local unit weight requirements are summarized in Table 4. It is concluded that the aerothermodynamic design of this concept is feasible using state-of-the-art technology.

Acknowledgment

This work was performed for the Jet Propulsion Laboratory of the California Institute of Technology, sponsored by the National Aeronautics and Space Administration under JPL Contract NAS 7-100.

The design concepts described in this paper were developed by the Re-entry Division of the General Electric Company under Contract No. 955344 for the Jet Propulsion Laboratory, California Institute of Technology. Manual Cruz was the JPL Project Monitor. The author expresses his appreciation to R.S. Neff of General Electric Company for his many helpful suggestions.

References

[1]Armento, R., "Mars Aerocapture Vehicle Definition Study Final Report," GE Report 79SDR2258, Aug. 1979.

[2]Repic, E.M., Boular, M.G., and Chapel, F.G., "Aerobraking as a Potential Planetary Capture Mode," *Journal of Spacecraft and Rockets*, Vol. 5, Aug. 1968, pp. 921-926.

[3]Cruz, M.I., Armento, R.F., and Giles, W.H., "Aerocapture—A System Design for Planetary Exploration," Paper No. 79-160, *30th International Astronautical Federation Congress*, Munich, Federal Republic of Germany, Sept. 16-22, 1979.

[4]Daywitt, J., Brant, D., and Bosworth, F., "Computational Technique for Three Dimensional Inviscid Flow Fields About Re-entry Vehicles," SAMSO-TR-79-5, April 1978.

[5]Hecht, A.M. and Nestler, D.E., "A Three-Dimensional Boundary Layer Computer Program for Sphere-Cone Type Re-entry Vehicles," AFFDL-TR-78-67, July 1978.

[6]Gentry, A.B., Smyth, D.N., and Oliver, W.R., "The Mark IV Supersonic-Hypersonic Arbitrary-Body Program," Vol. I, II, and III, AFFDL-TR-73-159, November 1973.

[7]Cline, P.B. and Schultz, F.B., "Investigation of the Effect of Material Properties on Composite Ablative Material Behavior," NASA CR-72142, April 1967.

[8]Berkowitz, A.M., Kyriss, C.L., and Martellucci, A., "Boundary Layer Transition Flight Test Observations," AIAA Paper No. 77-125, Jan. 1977.

[9]Florence, D., Thibault, H., and Hiltz, A., "Selection, Development, Characterization and Flight Test of a Thermal Protection System for an Earth Entry Satellite Vehicle," AIAA Paper No. 78-861, May 1978.

[10]Thuss, R.C., "Development of Low Cost Space Shuttle Thermal Protection Materials in Bulk Form," General Electric Space Division Final Technical Report NAS 9-13055, May 1973.

[11]Hiltz, A., "Exploratory Development of a Flexible Ablative Covering for Space Shuttle Application," NASA-CR-128502, June 1972.

[12]Hess, T.E. and Michalak, R.J., "Final Report for Reusable Surface Insulation Thermal Protection System Development Program," General Electric Space Division Final Technical Report NAS 9-12084, May 1972.